

Drying of Colloidal Binder Infiltrated Ceramic Green Parts Produced by Selective Laser SinteringTM

M. Glazer[†], N.K. Vail[‡], and J.W. Barlow[‡]

[†] Department of Mechanical Engineering

[‡] Department of Chemical Engineering

The University of Texas at Austin

Abstract

Colloidal ceramic binders have been used to strengthen ceramic green shapes produced by Selective Laser Sintering. This paper focuses on the effectiveness of the colloid infiltration with respect to the physical properties of the colloidal binder. Mass gains, strength gains, and dimensional changes resulting from infiltration were monitored. Controlled drying experiments were conducted to predict the factors influencing drying times for complex shapes.

(Key Words: Alumina, Silica Colloid, Drying)

Introduction

Ceramic preforms can be produced by Selective Laser Sintering of ceramic powders that have been encapsulated with a fugitive polymer binder. In this process, the polymer binder sinters producing a composite ceramic matrix. However, the polymer binder must be replaced because it does not have sufficient strength nor the thermal resistance necessary for functional ceramic objects. This paper discusses the infiltration of these preforms with ceramic colloids to improve strength and temperature capabilities. Green alumina coupons were infiltrated with colloids of varying solids content and then dried under controlled conditions. Physical properties of the coupons were determined prior to and following colloidal infiltration.

Materials

The polymer encapsulated ceramic used in this study is the same as that used in a previous study¹. This material consists of a high purity, electrical grade aluminum oxide, provided by Lanxide Corporation, coated with a polymethylmethacrylate polymer having a specified melt flow index of 20g/10min as measured by a Kayness Capillary Rheometer at 200°C and 75 psi (ASTM D1238). Figure 1 shows the mean particle size of the uncoated alumina to be 10.3µm, as measured by a Coulter Multisizer. The particles were observed to be regular in shape using a scanning electron microscope.

Samples of LudoxTM colloidal silica, grade TM, were provided by Dupont Corporation. This colloid is 50% wt. silica and consists of particles having a mean diameter of 22nm. A sample of Dupanol ME, a sodium dodecyl sulfate based emulsifier, was also provided by Dupont Corporation.

Methods

SLS Production of Test Coupons

Test specimens were produced using an SLS Model 125 workstation equipped with a 25 watt CO₂ laser. Fabrication of parts was conducted in an inert nitrogen environment using the

parameters listed in Table I. A number of rectangular coupons 1"x1"x0.25" (Group 1), 1"x1"x0.5" (Group 2), and 1.25"x1.25"x0.25" (Group 3) were produced for drying studies. Additional coupons 1"x3"x0.25" were produced for strength measurements. Densities of these coupons were determined by mass and dimensional measurements.

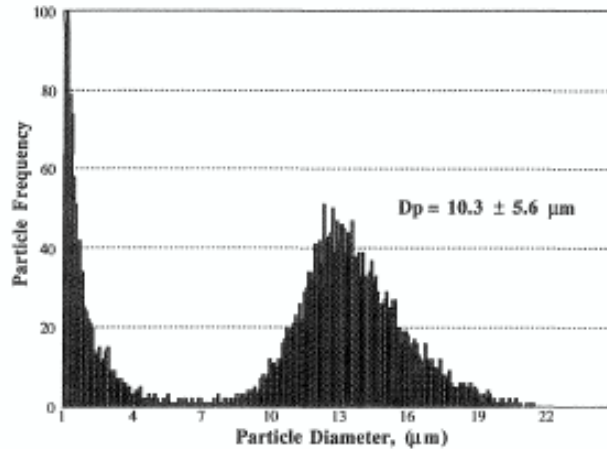


Figure 1. Particle size distribution of Lanxide alumina.

Table I. SLS parameters for test specimens used in this study.

Laser Power, (W)	Layer Thickness, (mil)	Beam Spacing, (mil)	Beam Speed, (ips)	Bed Temperature, (°C)
10	4	2	50-110	65

Post-processing of preforms

Each coupon size was infiltrated with colloids of varying silica content. The stock colloid was diluted with deionized water to produce samples with 10%, 20%, 30%, and 40% wt. silica. Emulsifier was added to each colloid sample to aid infiltration in an amount of 1.0% wt. based on total water content.

Infiltration was accomplished by placing a coupon in a pool of colloid and allowing it to draw up the colloid. When the colloid reached the top of the coupon additional colloid was dripped on to the top surface. The coupon was then transferred to a paper towel and excess colloid was drawn off. When no further colloid could be drawn off, colloid was dripped on the top of the coupon. Infiltration was considered complete when a wet spot appeared on the paper towel.

Following infiltration the coupons were weighed, measured, and transferred to a drying chamber. Figure 2 shows the constant humidity drying chamber used in this study. Temperature and relative humidity in the chamber were monitored with a thermohygrometer. Temperature was maintained at the room temperature of 24°C. Relative humidity was maintained at 64±2% with a sodium dichromate salt solution². An air flow rate of 45 ft/s, measured by a Alnor Velometer, was provided by an electric fan controlled by a rheostat. Laminar air flow was created by forcing the air through a group of narrow, adjacent tubes.

In the chamber, the coupons were placed on a platform suspended from a cantilever balance. The balance was connected to an LVDT which sent a signal to a data acquisition system. The initial and final masses of the sample provided the calibration of the LVDT. The data was used to observe the changing moisture content of the part as a function of time. After drying, the bars were removed from the chamber, weighed, measured, baked at 200°C for 1 hr. to remove residual water and then weighed again.

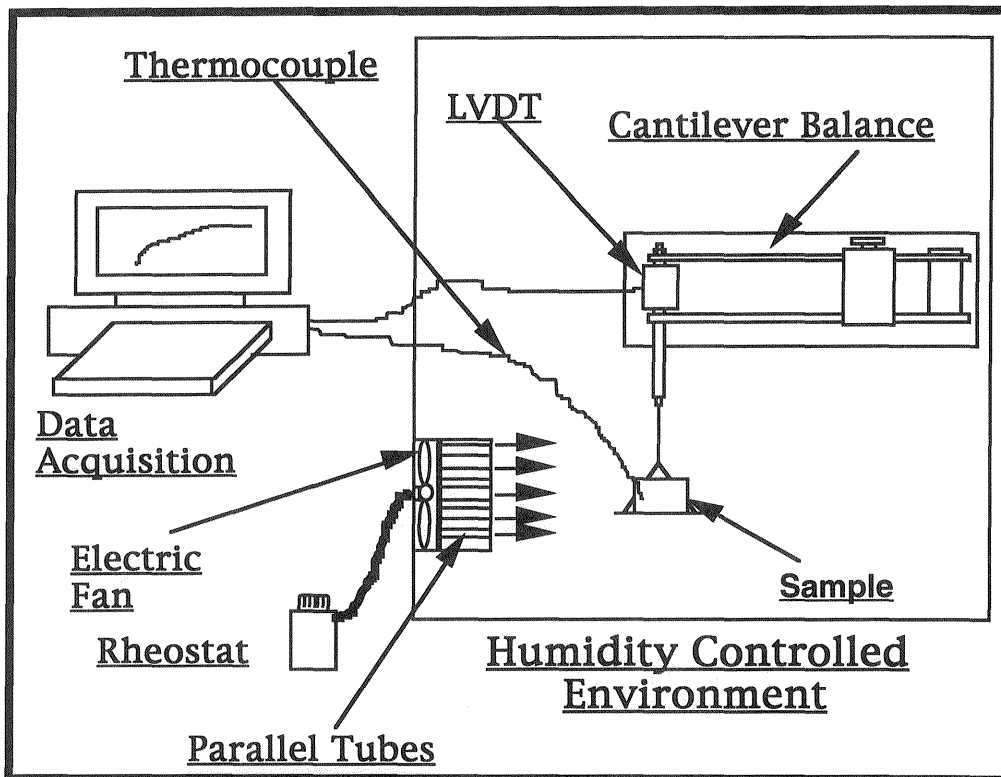


Figure 2. Drying chamber and data acquisition system.

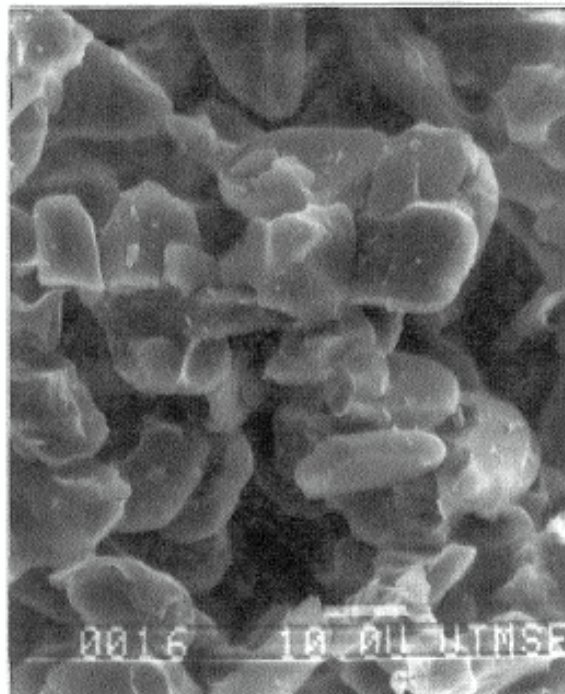
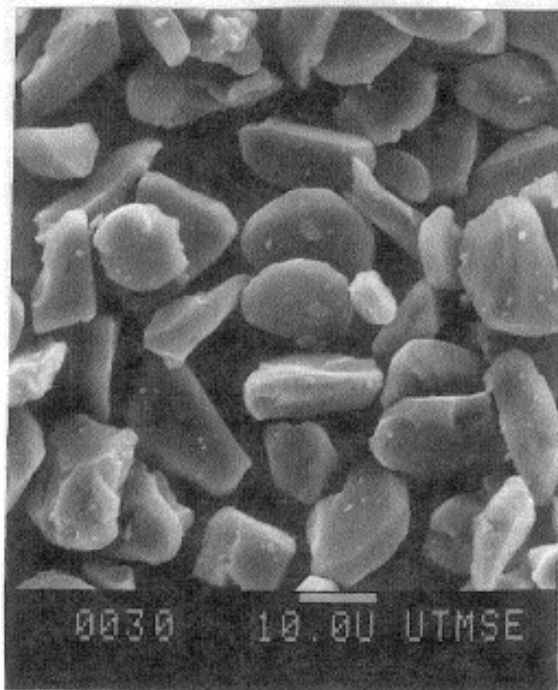


Figure 3. (left). Pure alumina powder. (right). Silica infiltrated alumina coupon with polymer removed by burnout at 400°C for 1 hour.

Results and Discussion

Prior to conducting drying tests, a set of experiments was performed to verify the effectiveness of the colloidal infiltration described above. This was done by introducing a dye into the colloid and observing cross-sections of wet coupons. Discoloration of cross-sections was observed to be homogeneous. Furthermore, x-ray mapping of cross-sections by scanning electron microscopy showed silica to be present at the center-line and a slight concentration gradient to exist. These two methods proved the infiltration method to be effective. Figure 2 shows SEM micrographs comparing pure alumina powder to silica infiltrated alumina. The figures clearly show an accumulation of material in the infiltrated sample.

Figure 4 shows resultant densities of square coupons. Prior to colloid infiltration, all coupons had an initial density of approximately 1.55g/cm^3 . As would be expected coupon density increases with increasing silica content in a nearly linear fashion. From mass balance considerations the observed increases in density are a result of silica infiltration. Dimensional fluctuations of the processed coupons were within experimental error with most exhibiting no more than 0.5% deviations.

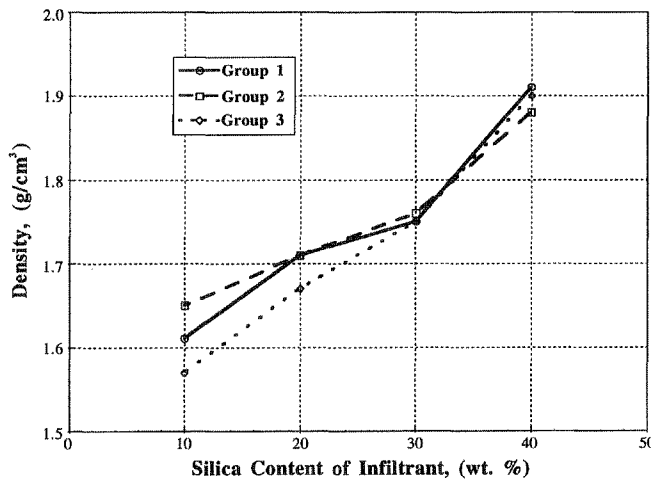


Figure 4. Density of test bars baked at 200°C .

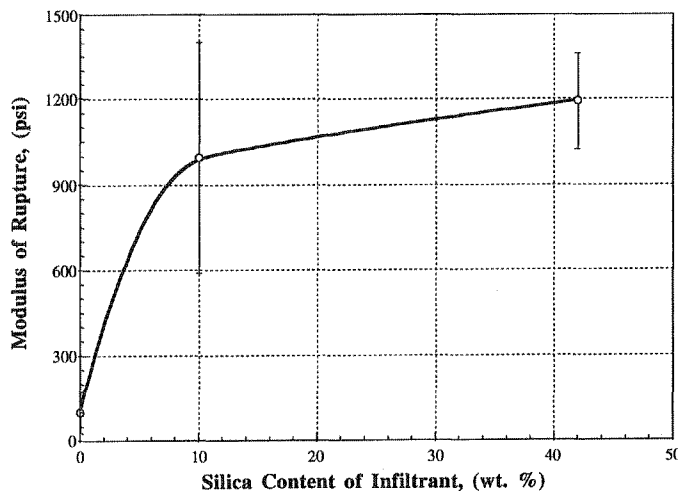


Figure 5. 3-point bend breaking strength of test coupons after baking at 200°C .

Figure 5 shows the modulus of rupture of test coupons which have been infiltrated, dried, and baked at 200°C for 1 hr.. Colloids that were 10 and 42 wt.% silica were used to determine the strengths which could be obtained by infiltration. The data shows a large gain in the green strength which appears to be independent of the amount of silica beyond 10 to 15 wt.% silica.

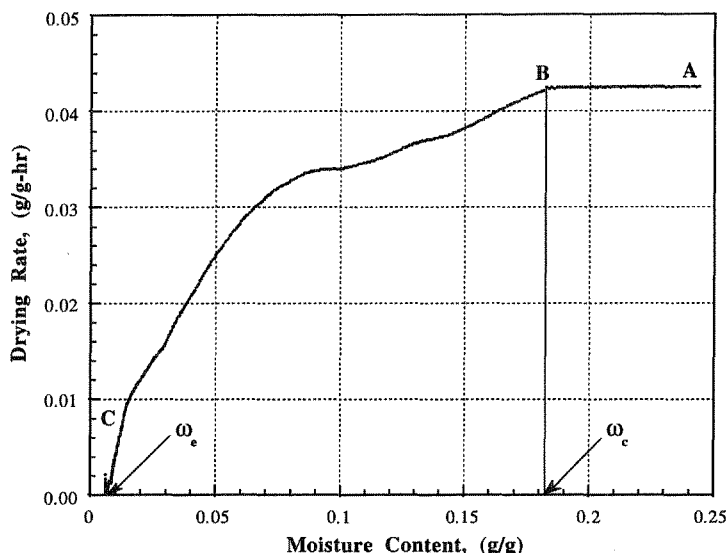


Figure 6. Drying data from infiltrated bar placed in drying chamber.

Figure 6 shows a typical drying curve for a coupon. This curve is similar to drying patterns observed by other authors and is indicative of drying of a hygroscopic material³. The rate curve is characterized by the constant rate period (AB) and the falling rate period (BC). During the constant rate period equilibrium of the drying surface is maintained by diffusion of excess moisture to the surface. At the critical moisture content, ω_c , the rate falls as the drying front recedes into the part. Analysis of these curves for the coupons studied here indicate the drying rate to be influenced by both coupon thickness and the solids content of the infiltrant. Using the analysis of Perry and Green⁴, it was determined that the drying process is controlled by diffusion and capillary moisture transport. A rigorous analysis of the data is in progress.

Cracking of coupons was observed to increase as the thickness of the part increased. Cracking also increased as the solids content of the infiltrant increased. In a separate set of experiments, coupons, that were infiltrated with water then dried under similar conditions, did not develop cracks. Cracking appears to be related to stresses induced by drying of the colloid and to the initial strength of the green coupon. Scherer⁵ has shown that ceramic colloids tend to shrink and crack during controlled drying. Therefore, as the drying front proceeds in to the coupon, stress gradients that exceed the green strength of the coupon may develop. Thicker coupons would necessarily experience larger stress gradients and be more likely to crack.

To examine the influence of initial green strength a set of coupons with similar dimensions but with different strengths were processed. Coupons having strengths of 45psi, 100psi, and 160psi were infiltrated with 30 wt. % colloid and dried under similar conditions. The low strength bar cracked severely, the high strength bar did not crack, and the moderate strength bar developed hairline cracks.

Conclusions/Further Work

Infiltration with silica colloids is an effective method for increasing strength and density of polymer bound prototypes produced by Selective Layer Sintering. Strength gains of the coupons were nearly independent of the solids content of the infiltrant. However, high solids infiltrants increased cracking, especially in parts with low inherent green strength.

Further study is required to optimize the infiltration and drying processes. Additional strength measurements need to be conducted on coupons from which the polymer binder has been removed. It may be necessary to subject the coupons to an additional colloid infiltration following binder removal to further increase density and strength. The strength of fired bars need to be studied, also.

A detailed analysis of stresses during the drying period, which includes the contributions of capillary and diffusion induced drying, is in progress. Infiltration with other ceramics could provide improved strength, temperature, and drying characteristics.

Acknowledgments

The authors gratefully acknowledge support of this work by the University of Texas SFF Industrial Associates Program.

References

1. N.K. Vail and J.W. Barlow, "Ceramic Structures by Selective Laser Sintering of Microencapsulated, Finely Divided Ceramic Materials," *Solid Freeform Fabrication Symposium Proceedings*, 3 (1992), pp. 124-130..
2. A. Wexler and S. Hasegawa, "Relative Humidity-Temperature Relationships of Some Saturated Salt Solutions in the Temperature Range 0° to 50°C," *Journal of Research of the National Bureau of Standards*, vol. 53, no. 1 (1954), pp. 19-25.
3. C. Strumillo and T. Kudra, *Drying: Principles, Applications and Design*, Gordon and Breach Science Publishers, Switzerland (1986), pp. 69-97.
4. R.H. Perry and D. Green, *Perry's Chemical Engineering Handbook*, 6th ed., McGraw-Hill, St. Louis (1984), pp. 20.9-20.14.
5. G.W. Scherer, "Drying Gels," *Journal of Non-Crystalline Solids*, 87 (1986), pp. 199-225.